

Article

# Alteration of Granitoids and Uranium Mineralization in the Blatná Suite of the Central Bohemian Plutonic Complex, Czech Republic

Miloš René

Institute of Rock Structure and Mechanics v.v.i, Academy of Sciences of the Czech Republic,  
180 09 Prague 8, Czech Republic; rene@irms.cas.cz

Received: 3 August 2020; Accepted: 16 September 2020; Published: 17 September 2020



**Abstract:** The Bohemian magmatic complex belongs to granitoid plutons of the Central European Variscides. Hydrothermal uranium mineralization evolved in the small uranium deposits Nahošín and Mečichov is associated with N–S shear zones occurring on the SW margin of the Central Bohemian plutonic complex formed by amphibole-bearing biotite granodiorites of the Blatná suite. The purpose of presented study is description of uranium mineralization bounded on brittle shear zones, which is coupled with intense low-temperature hydrothermal alteration of granitic rocks. Uranium mineralization, formed predominantly of coffinite, rare uraninite, and thorite, is accompanied by intense hematitization, albitization, chloritization, and carbonatization of original granitic rocks that could be described as aceites. These alterations are accompanied by the enrichment in U, Ti, Mg, Ca, Na, K, Y, and Zr and depletion in Si, Ba, and Sr. The analyzed coffinite is enriched in Y (up to 3.1 wt %  $Y_2O_3$ ). Uraninite is enriched in Th (up to 9.8 wt %  $ThO_2$ ) and thorite is enriched in Zr (up to 5.7 wt %  $ZrO_2$ ). The REE-elements are concentrated in the REE-fluorcarbonate synchysite-(Ce).

**Keywords:** uranium mineralization; aceite; coffinite; uraninite; thorite; synchysite; mineralogy; geochemistry; Bohemian Massif; Central European Variscides

## 1. Introduction

The Bohemian Massif as a part of the European Variscan belt hosts a significant quantity of vein-type uranium deposits (Aue/Oberschlema, Příbram, and Jáchymov) and uranium deposits coupled with brittle shear zones developed in high-grade metamorphic rocks (Rožná, Zadní Chodov, and Okrouhlá Radouň) and/or in S-type granitic rocks (Vítkov II and Okrouhlá Radouň) [1–7]. The small uranium deposits Nahošín and Mečichov described in a recent paper are good examples of uranium deposits coupled with shear zones which are accompanied by extensive low-temperature hydrothermal alterations, usually described as episyenites [8–10] and/or as aceites [11,12]. The aim of this paper is to provide a detailed study of mineralogy and geochemistry of U-Th-REE mineralization evolved in the I-type granitic rocks of the Central Bohemian plutonic complex.

## 2. Geological Setting

The Central Bohemian plutonic complex is a large composite magmatic body that occupies an extensive area (3200 km<sup>2</sup>) between Prague and Klatovy. This plutonic complex represents in its composition petrographically the most differentiated Variscan magmatic body on the Bohemian Massif (Figure 1). The most widespread rock types of the plutonic complex are hornblende-biotite granites and granodiorites, accompanied by biotite granites on one hand and by tonalites and melagranites along with melasyenites (durbachites) on the other. Gabbro's and gabbrodiorites along with a wide

suite of dyke rocks of predominantly intermediate to mafic composition (microgabbros, microdiorites, and lamprophyres) emphasize the diversity of this plutonic complex [13–15].

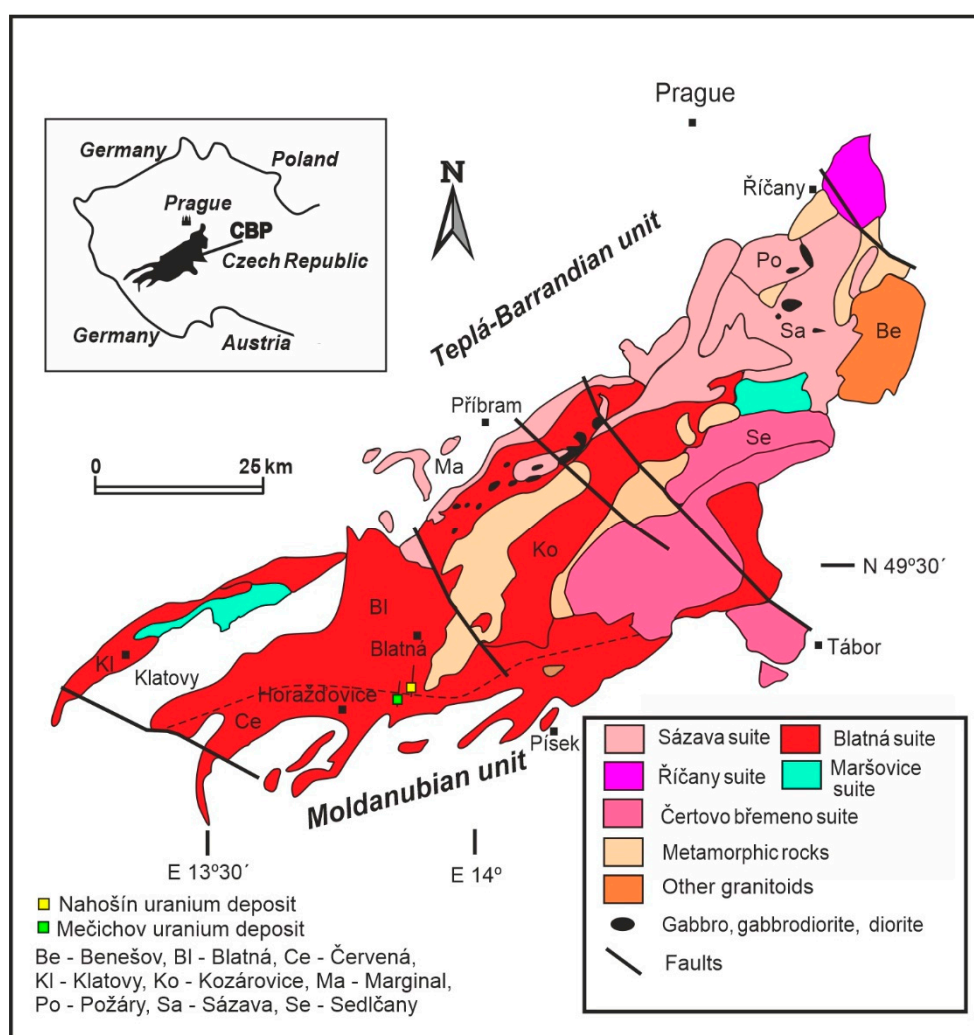


**Figure 1.** Geologic map of the Central Bohemian plutonic complex, modified from [13].

The uranium deposits Nahošín and Mečichov are situated in the amphibole-bearing biotite granodiorites of the Blatná suite, especially in the Blatná granodiorites (Nahošín) and in the Červená granodiorites (Mečichov) [16–19]. The Blatná suite occurs in the southern and southwestern margin of the Central Bohemian plutonic complex. The Blatná suite is formed by more petrographic rock types (Klatovy, Kozárovce, Blatná and Červená granites, granodiorites, and tonalites) [13,14,20,21] occurring in the southern and southwestern margin of the Central Bohemian plutonic complex. The most common rock type of the Blatná suite, occurring in area of the both uranium deposits, is an amphibole-biotite granodiorite, with the modal content of amphibole gradually decreasing inwards [22]. These granitoids intruded during the Variscan magmatic event ( $346.7 \pm 1.6$  Ma, U/Pb TIMS analyses on zircon) [14]. To the south and south-eastern, the Blatná granodiorite grades in the Červená granodiorite, this is richer in amphibole (up 2 vol. %).

The uranium deposits Nahošín and Mečichov were found as one of the last explored uranium deposits in the Czech Republic during geological mapping, radiometric exploration, and following extensive borehole exploration (150–500 m) (1978–1989) performed by the exploration organization of the Czechoslovak Uranium industry (ČSUP) [16–19]. During the exploration activity a low-grade uranium mineralization associated with the N–S shear zones, was found (Figure 2). The concentration

of uranium in these shear zones is 0.01–0.5 wt % U [16]. The origin of the N–S shear zones could be correlated with the Variscan post-orogenic extension of the central part of the Bohemian Massif during the Late Westphalian and Stephanian (307–300 Ma) [1,5]. The total approved prognostic resources of the both deposits were estimated as 1824 t U [23]. The uranium deposit Nahošín was in 1983 opened by exploration shaft Nr. 82 down to level 190 m. During 1987 and 1988 this uranium deposit was mined with a total production of 4.2 t U [24]. Investigations connected the exploration activity of the ČSÚP were concentrated only on detailed geological and mineralogical study of uranium mineralization [16–19]. For this research, samples were taken from three boreholes performed in area of the Nahošín uranium deposit and from six boreholes performed in area of the Mečichov uranium deposit. The metasomatic uranium mineralization of the both deposits is represented mainly by two generations of coffinite, with a small content of uraninite. The U/Pb age of primary coffinite mineralization is  $280 \pm 10$  Ma with partial rejuvenation around  $165 \pm 20$  Ma [19] (Figure 2).

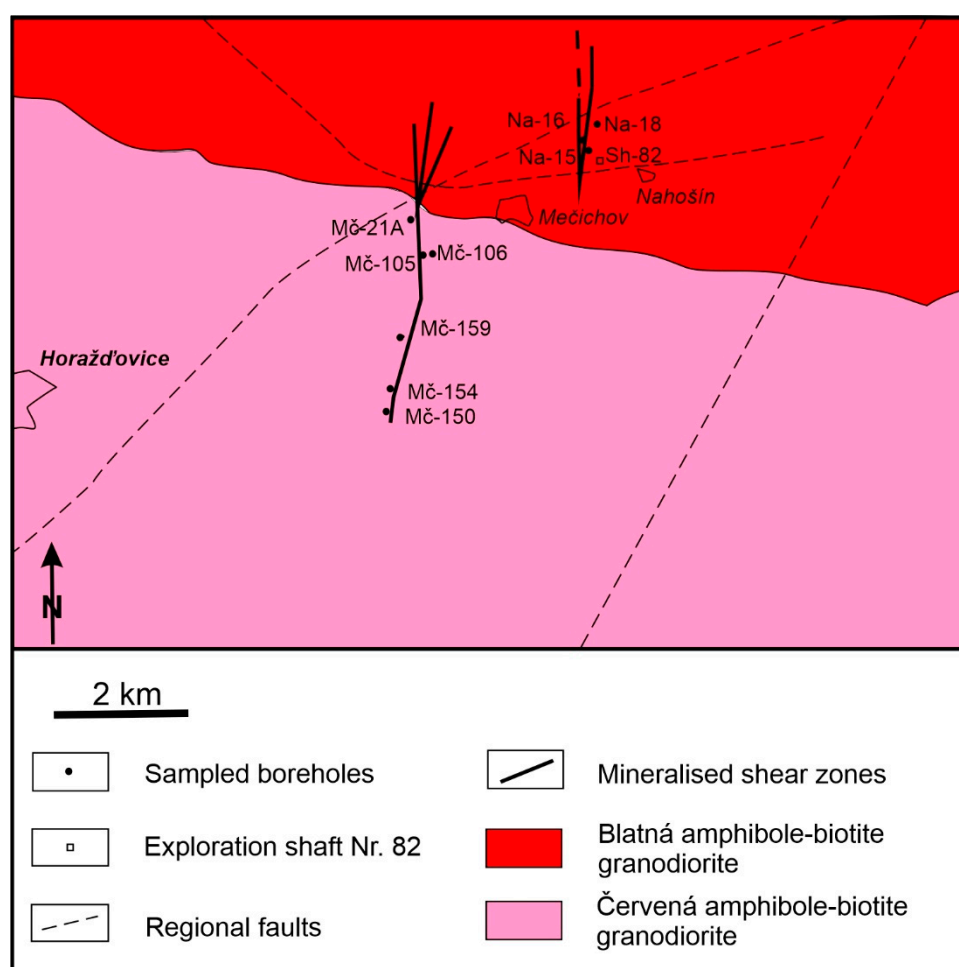


Figure 2. Schematic geological map of the Nahošín and Mečichov uranium deposits, modified from [17].

### 3. Materials and Methods

Detailed mineralogical and geochemical investigations of uranium mineralization from the Nahošín and Mečichov uranium deposits were carried out on a representative suite of the 31 rock samples were taken from exploration boreholes performed by ČSÚP during their exploration activity in the area of the both uranium deposits. These samples represent unaltered host granitic rocks, as well as their hydrothermally altered equivalents (Table S1).

The major elements were determined by X-ray fluorescence spectrometry using the Philips PW 1410 spectrometer at the Central Analytical Laboratory of the ČSÚP. The FeO content was measured

via titration, whereas the H<sub>2</sub>O content was determined gravimetrically. The selected trace elements were determined by X-ray fluorescence spectrometry using the Philips PW 1410 spectrometer at the chemical laboratory of the Unigeo Brno Ltd. (Brno, Czech Republic). The content of U and Th was determined by gamma spectrometry using a multi-channel spectrometer NT-512 at Geophysics Brno Ltd. (Brno, Czech Republic). In-lab standards or certified reference materials were used for quality control. The elemental mobility during hydrothermal alteration was estimated using mass-balance calculations of selected representative rock samples based on the isocon method [25].

Representative rock-forming and ore minerals were analyzed in polished thin sections, and back-scattered electron (BSE) images were acquired to study the internal structure of individual mineral aggregates and grains. The elemental abundances of Al, As, Ca, Ce, Cu, Cr, Dy, Er, F, Fe, Gd, Hf, La, K, Mg, Mn, Na, Nb, Nd, P, Pb, Pr, Rb, S, Sc, Si, Sm, Sr, Ta, Th, Ti, U, V, Y, Yb, and Zr were determined using a CAMECA SX 100 electron microprobe operated in wavelength-dispersive mode at the Institute of Geological Sciences, Masaryk University in Brno. The accelerating voltage and beam currents were 15 kV and 20 nA or 40 nA, respectively, and the beam diameter was 1 to 5  $\mu\text{m}$ . The peak count time was 20 s, and the background time was 10 s for major elements. For the trace elements, the times were 40–60 s on the peaks, and 20–40 s on the background positions. The raw data were corrected using the PAP matrix corrections [26]. The detection limits were approximately 400–500 ppm for Y, 600 ppm for Zr, 500–800 ppm for REE, and 600–700 ppm for U and Th.

## 4. Results

### 4.1. Petrography of the Blatná and Červená Granitoids

The Blatná hornblende-bearing biotite granodiorites are medium-grained, usually equigranular rocks, containing 12–18 vol. % of biotite (phlogopite–eastonite, Fe/Fe + Mg 0.48–0.51, Al<sup>4+</sup> 2.4–2.6 apfu, Ti 0.20–0.43 apfu), 40–42 vol. % plagioclase (An<sub>23–31</sub>), 25–28 vol. % quartz, 10–17 vol. % K-feldspar, and 0.2–0.7 vol. % amphibole (magnesianhornblende) (Figure 3a). In a relatively rarely occurring porphyric variety of this rock type, the size of K-feldspar variety reaches 1–2 cm. Accessory minerals are represented by apatite, zircon, titanite, magnetite, pyrite, and rare allanite. The highest content of U occurred in zircon (0.08–0.34 wt % UO<sub>2</sub>) and the highest content of Th occurred in allanite (0.08–6.37 wt % ThO<sub>2</sub>). The highest content of Y is in titanite (0.05–1.29 wt % Y<sub>2</sub>O<sub>3</sub>) and in allanite (0.06–0.61 wt % Y<sub>2</sub>O<sub>3</sub>).

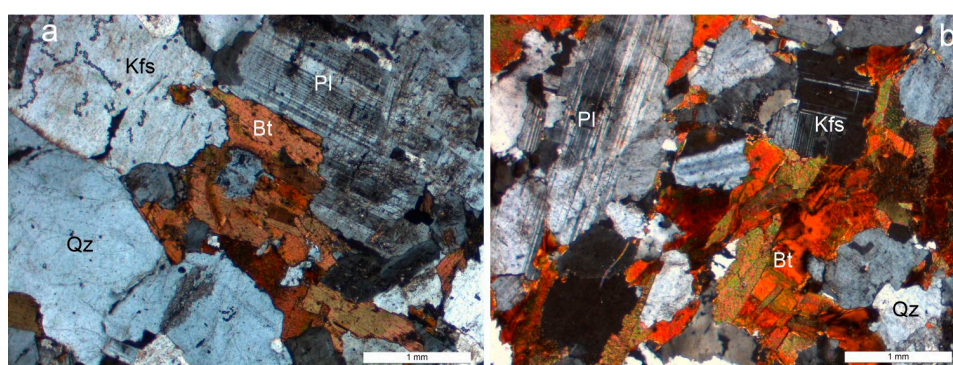


**Figure 3.** Microphotographs of the Blatná (a) and the Červená granodiorites (b) (Bt—biotite, Kfs—K-feldspar, Pl—plagioclase, and Qz—quartz). Crossed polarizers.

The Červená amphibole-biotite granodiorites are medium-grained, equigranular to slightly porphyric rocks, containing 15–17 vol. % biotite (eastonite, Fe/Fe + Mg 0.44–0.47, Al<sup>4+</sup> 2.5–2.6 apfu, Ti 0.28–0.38 apfu), 28–41 vol. % plagioclase (An<sub>22–40</sub>), with usually more basic cores than their rims, 22–23 vol. % quartz, 9–19 vol. % K-feldspar, and 1–2 vol. % amphibole (magnesianhornblende,

actinolite) (Figure 3b). Accessory minerals are represented by apatite, zircon, titanite, magnetite, allanite, and pyrite. These granitoids have in some cases a strong planar fabric.

#### 4.2. Petrography of Altered Granitoids

The three major stages of alteration of the Blatná and Červená granodiorites can be distinguished, namely pre-ore, ore and post-ore stages. The presented paragenetic sequence of the hydrothermal mineralization is partly schematic. In altered granitoids chlorites, albites, hematites, and carbonates (calcites) are dominant, whereas coffinite, uraninite, thorite, Ti-oxides and sulfides (pyrite and chalcopyrite) are less abundant. The highly altered granodiorites could be classified as aceites (Figure 4).

Stage	Pre-ore	Ore	Post-ore
Chlorite	I		II
Sericite			
Apatite			
Rutile, Titanite			
Quartz			
Albite			
K-feldspar			
Calcite			
Pyrite			
Hematite			
Coffinite			
Uraninite			
Thorite			
Chalcopyrite			
Clausthalite			
Galenite			
Clay minerals			
Synchysite			

**Figure 4.** Paragenetic sequence of the hydrothermal mineralization of the Nahošín and Mečichov uranium deposits, modified from [19].

During pre-ore alteration of biotite granodiorites, original biotite was chloritized and altered to chlorite I ( $\text{Fe}/(\text{Mg} + \text{Fe}) = 0.46\text{--}0.51$ ). Alteration of biotite is commonly accompanied by formation of rutile, epidote, and titanite due to the liberation of Ti from original biotite laths. Original magmatic plagioclases ( $\text{An}_{22\text{--}40}$ ) were transformed into albite ( $\text{An}_{0.1\text{--}0.6}$ ) (Figure 5). Albitization is sometimes accompanied by K-feldspathization, coupled with formation of usually anhedral grains of K-feldspar (Figure 6). This K-feldspathization is sometimes accompanied by sericitization. More intensive

hydrothermal alteration of original granitoids is significant for the origin of fine-grained aggregates of hematite that occur as very fine grains and/or grain aggregates in albites (Figure 7). These hydrothermal alterations, documented by detailed microscopic study, predated the origin of uranium mineralization. Hydrothermally altered granitoids have low to medium porosities due to hydrothermal leaching of the original magmatic quartz (typically 0.5–5 vol. %) and partly lowered specific mass (approximately 0.10–0.20 g/cm<sup>3</sup>). The vugs formed initially through leaching of quartz were later infilled by a younger K-feldspar, quartz, calcite, and chlorite II (Figures 5 and 6). Hydrothermal alteration of granitoids is also accompanied by origin of younger apatite, often associated with coffinite. During post-ore stage, the altered granitoids were filled by variable thick and irregular calcite veinlets (Figure 5a). In altered granodiorites from these uranium deposits these veinlets are sometimes filled by fine-grained aggregates of the REE-fluorocarbonate synchysite-(Ce), which usually contain inclusions of very small thorite grains (Figure 8a,b). The origin of these veinlets is very probably also coupled with the post-ore stage. However, partly unclear is timing of thorite. The individual thorite grains (Figure 8e) are very probably part of the ore stage, but the small thorite grains in aggregates of the synchysite (Figure 8a) could be partly younger. During post-ore stage originated clay minerals (illite, kaolinite, and smectite), together with younger sericite.

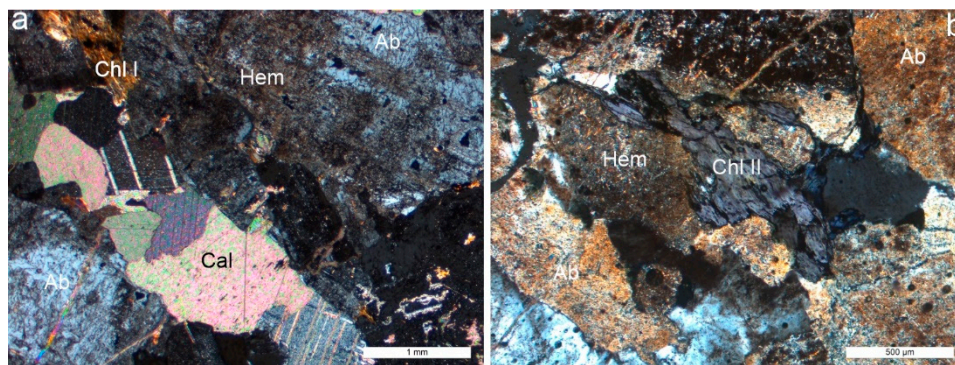


**Figure 5.** Microphotographs of hydrothermally altered granitoids (Ab—albite, Cal—calcite, Chl—chlorite, and Hem—hematite), (a)—Nahošín uranium deposit, sample R-752; (b)—Mečichov uranium deposit, sample R-784. Calcite usually occur in small veins and veinlets. Albite is enriched by very fine hematite grains. Chlorite I originated by alteration of biotite. During post-ore stage originated sometimes chlorite II. Crossed polarizers.

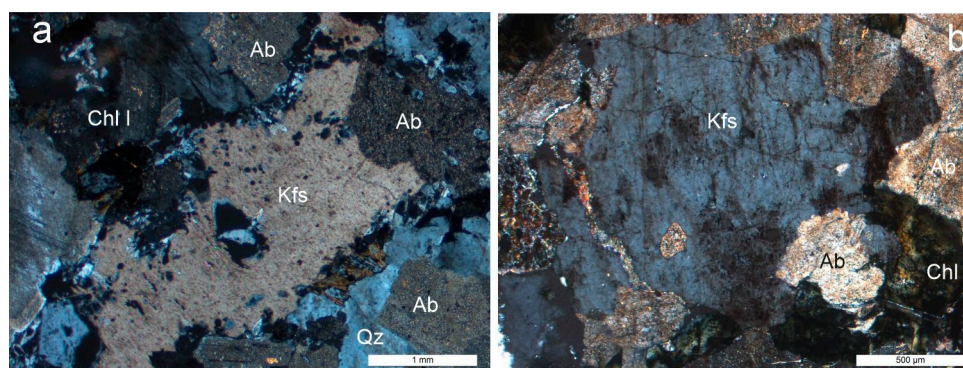


**Figure 6.** Microphotographs of hydrothermally altered granitoids (Ab—albite, Chl—chlorite, Kfs—K-feldspar, and Qz—quartz) with hydrothermally originated K-feldspars during K-feldspathization, Nahošín uranium deposit, (a)—sample R-707; (b)—sample R-705. Crossed polarizers.

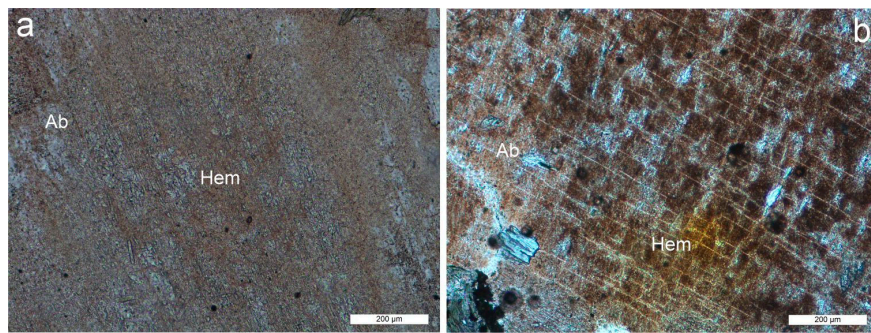


**Figure 7.** Microphotographs of hematized albite (Ab—albite and Hem—hematite), (a)—very fine hematite grains uniformly distributed in albite, sample R-707, Nahošín uranium deposit, (b)—hematite aggregates irregularly distributed in albite, sample R-784, Mečichov uranium deposit. Plane polarizers.

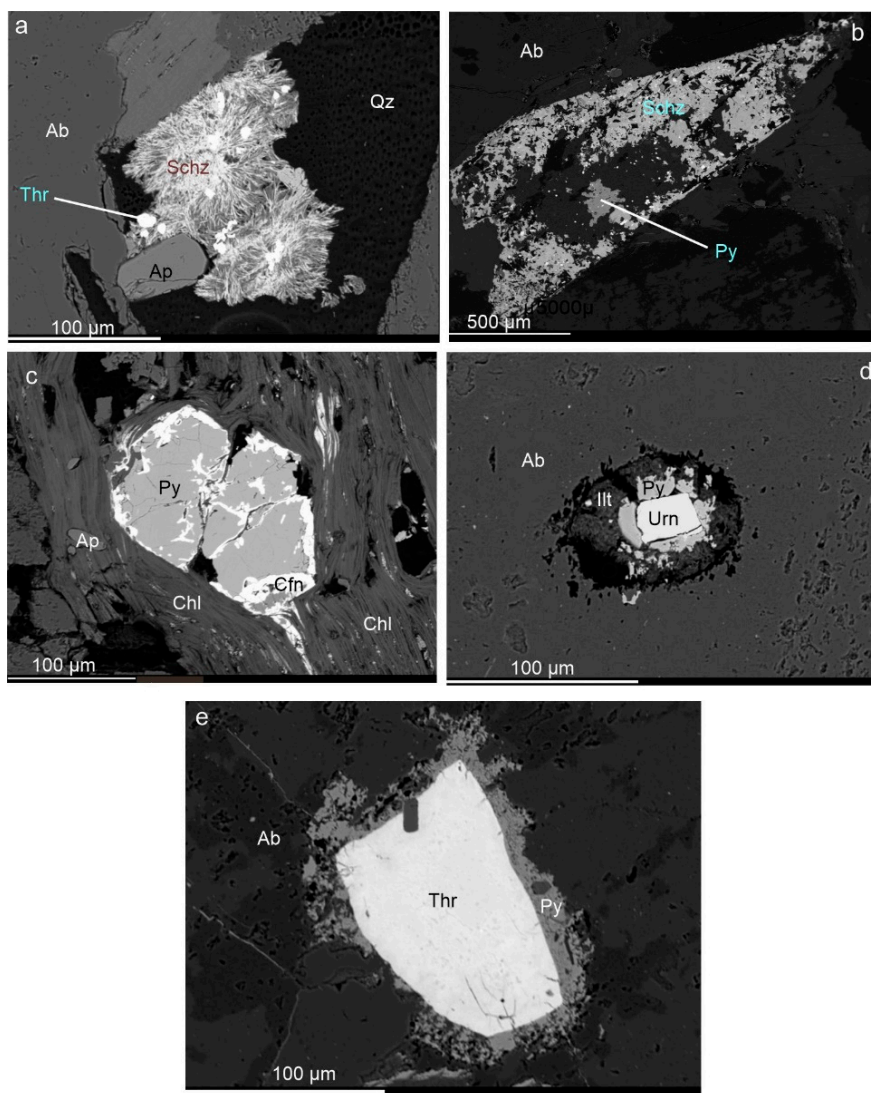


**Figure 8.** Back-scattered electron (BSE) images of coffinite, synchysite, thorite, and uraninite occurring in hydrothermally altered granodiorites (Ab—albite, Ap—apatite, Cfn—coffinite, Chl—chlorite, Ill—illite, Qz—quartz, Py—pyrite, Schz—synchysite, Thr—thorite, and Urn—uraninite), (a)—Nahošín uranium deposit, sample R-710; (b)—Mečichov uranium deposit, sample R-784; (c)—Nahošín uranium deposit, sample R-752; (d)—Nahošín uranium deposit, sample R-710; and (e)—Mečichov uranium deposit, sample R-784.

#### 4.3. Chemical Composition of Unaltered Granitoids

The representative chemical analyses of the unaltered and altered granodiorites are displayed in Table 1. The Blatná amphibole-bearing biotite granodiorites are high-K calc-alkaline to shoshonitic, subaluminous to slightly peraluminous rocks ( $A/CNK = \text{mol. Al}_2\text{O}_3/(\text{CaO} + \text{Na}_2\text{O} + \text{K}_2\text{O}) = 1.1\text{--}1.2$ ). Compared to the common I-type granites [27,28], the Blatná granodiorites are enriched in Mg (1.2–1.7 wt % MgO), K (3.7–4.2 wt % K<sub>2</sub>O), Ba (1044–1284 ppm), Sr (383–506 ppm), Zr (135–172 ppm), Th (14–21 ppm), and U (7–14 ppm). The Červená amphibole-biotite granodiorites are also high-K calc-alkaline I-type, metaluminous to subaluminous rocks ( $A/CNK = 1.0\text{--}1.1$ ), enriched in Ca (1.5–3.5 wt % CaO), Mg (2.1–3.4 wt % MgO), Ba (1119–2560 ppm), Sr (261–466 ppm), Zr (164–231 ppm), Th (14–23 ppm), and U (8–14 ppm).

**Table 1.** Representative chemical analyses of rocks from the Nahošín and Mečichov uranium deposits.

Sample	R-704	R-709	R-780	R-986	R-710	R-752	R-781	R-981
	Nahošín	Nahošín	Mečichov	Mečichov	Nahošín	Nahošín	Mečichov	Mečichov
Rock wt %	amf-bt gnt	amf-bt gnt	amf-bt gnt	amf-bt nt	altered gnt	altered gnt	altered gnt	altered gnt
SiO <sub>2</sub>	69.52	68.87	63.38	62.11	59.28	43.65	53.52	58.97
TiO <sub>2</sub>	0.60	0.58	0.71	0.79	0.62	0.42	0.73	0.39
Al <sub>2</sub> O <sub>3</sub>	15.66	15.63	16.02	16.87	15.44	14.92	18.86	16.20
Fe <sub>2</sub> O <sub>3</sub>	0.01	0.44	0.80	0.74	1.30	1.53	2.22	1.00
FeO	2.08	1.80	3.55	4.08	1.80	1.42	2.48	1.94
MnO	0.04	0.05	0.07	0.08	0.10	0.12	0.09	0.05
MgO	1.27	1.19	2.65	3.00	1.74	2.26	3.20	1.88
CaO	1.98	2.36	3.25	3.68	5.25	14.40	3.85	4.23
Na <sub>2</sub> O	3.26	3.58	3.06	2.95	3.73	3.46	4.28	5.38
K <sub>2</sub> O	4.20	3.98	4.11	3.55	4.12	3.55	4.91	4.25
P <sub>2</sub> O <sub>5</sub>	0.30	0.36	0.26	0.25	0.42	0.20	0.28	0.17
H <sub>2</sub> O <sup>+</sup>	0.83	0.81	0.86	1.00	1.29	1.33	1.82	1.42
H <sub>2</sub> O <sup>−</sup>	0.00	0.00	0.20	0.00	0.02	0.33	0.63	0.16
CO <sub>2</sub>	0.14	0.12	0.14	0.00	4.49	11.30	2.64	3.38
Total	99.89	99.77	99.06	99.10	99.60	98.89	99.51	99.42
A/CNK	1.26	1.08	1.04	1.10	0.77	0.42	0.97	0.77
ppm								
Ba	1165	1144	1562	1400	1191	659	1368	1710
Rb	161	146	101	128	211	160	157	100
Sr	410	453	466	427	320	185	233	276
Nb	11	8	11	12	24	22	13	17
Zr	150	141	223	236	166	322	205	195
Y	23	23	29	20	45	33	29	11
Pb	51	55	48	27	68	39	34	35
U	9	8	8	3	366	378	11	391
Th	18	20	15	14	16	20	24	28

#### 4.4. Chemical Composition of Altered Granitoid Rocks

Hydrothermal alteration of the Blatná and Červená granodiorites is accompanied by silica removal from quartz and biotite. Concentrations of Al<sub>2</sub>O<sub>3</sub> and Fe<sub>2</sub>O<sub>3</sub> increased during the albitization, chloritization, sericitization, and hematitization. In intensively hematitized granitoids from the Mečichov uranium deposit the content of Fe<sub>2</sub>O<sub>3</sub> reaches up to 3.3 wt %. The content of Ca distinctly increases in altered granodiorites due to their, usually intensive carbonatization, reaching up to 14.4 wt % CaO in aegirites from the Nahošín uranium deposit. The content of Na increases especially in altered granodiorites from the Mečichov uranium deposit, affected by a strong albitization (up to 5.4 wt % Na<sub>2</sub>O). In altered granodiorites affected by K-feldspathization, there are distinctly increased K concentrations (up to 6.2 wt % K<sub>2</sub>O). These granodiorites are also enriched on Rb. The highest

concentrations of Rb were found in aceites from the Nahošín uranium deposit (up to 214 ppm). In the same aceites depletions in Sr were found (79–383 ppm). In unaltered granodiorites from the Nahošín uranium deposit the concentrations of Rb and Sr are 138–166 ppm and 383–506 ppm, respectively (Figure 9). The altered granodiorites from the Nahošín uranium deposit are also concentrations of Y enriched, reaching up to 45 ppm. Its concentrations in unaltered granodiorites from the Nahošín uranium deposit are only 21–36 ppm.

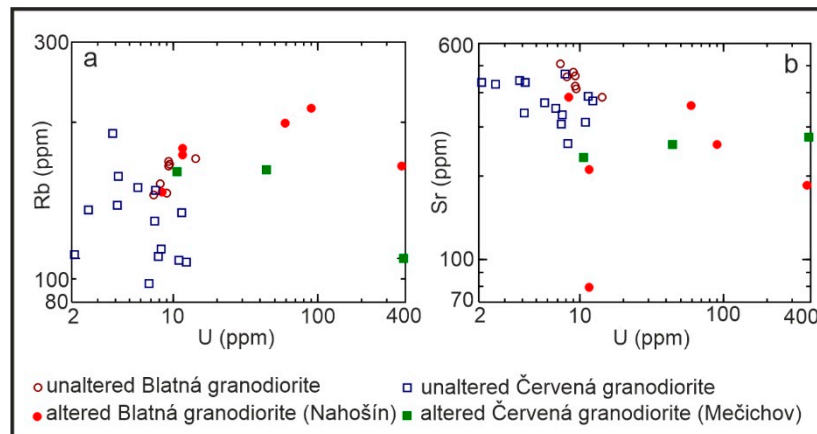


**Figure 9.** Plots of distribution Rb and Sr in unaltered and altered granodiorites of the Nahošín and Mečichov uranium deposits. (a) Distribution Rb vs. U, (b) Distribution Sr vs. U.

However, where significant mass or volume change occurred during hydrothermal alteration, the chemical composition of the unaltered and altered rocks cannot be compared directly. Thus, for the detailed investigation of losses and gains during alteration and the behavior of selected rock-forming and trace elements, the isocon method developed by Grant [25] was applied. The resulting scattering of elements in the isocon plots for the Blatná a Červená altered granodiorites from area of the Nahošín and Mečichov uranium deposits suggest that the major and trace elements were mobilized to variable extent. It appears that the sample of aceite from the Nahošín uranium deposit is a highly hematitized and carbonatized (Figure 10a), whereas the aceite sample from the Mečichov uranium deposit is not as altered (Figure 10b). In the both cases,  $\text{Al}_2\text{O}_3$  could be considered as an immobile component. In a well-studied sample from the Nahošín deposit, Zr and Y are distinctly enriched and accumulated in uranium minerals (uraninite and coffinite). In sample from the Mečichov uranium deposit, Zr and Y are depleted and Th is distinctly enriched. The differences between both isocon plots are coupled with differences in composition of unaltered granitic rocks and by some differences in hydrothermal alterations (distinctly higher hematitization and carbonatization in the case of sample R-752 from the Nahošín ore deposit).

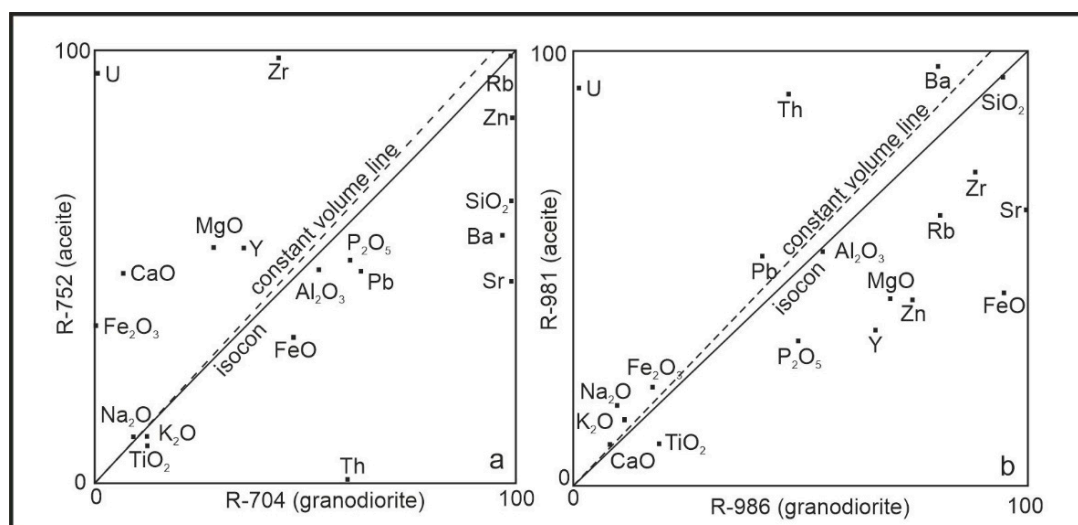


**Figure 10.** Isocon plot of the altered granodiorites (aceites) vs. unaltered granodiorites of the Blatná suite, (a)—Nahošín uranium deposit; (b)—Mečichov uranium deposit.

#### 4.5. Composition of Uranium and Thorium Minerals

The predominant uranium mineral occurring in altered granodiorites of the Nahošín and Mečichov uranium deposits is coffinite. Uraninite occurs in both uranium deposits as a rare uranium mineral; in altered granites from these both uranium deposits thorite occurs as very rare mineral.

The coffinite occurs in altered granodiorites of both the uranium deposits as distinctly heterogeneous aggregates and/or as isolated grains of some micrometers to 0.6 mm big, usually associated with chlorite flakes and/or associated with pyrite grains (Figure 8c). Some coffinite grains occur as filling of micropores in highly altered granodiorites. For all analyzed coffinites there is a strong correlation between  $\text{SiO}_2$  and  $\text{UO}_2$  with U/Si relations 0.63–0.80 (Figure 11). The majority of analyzed coffinites are distinctly enriched in  $\text{Y}_2\text{O}_3$  (up to 3.3 wt %) (Table 2). The microprobe data revealed variable CaO (1.4–2.3 wt %),  $\text{Al}_2\text{O}_3$  (1.5–2.0 wt %),  $\text{TiO}_2$  (0–1.3 wt %),  $\text{P}_2\text{O}_5$  (0.1–0.3 wt %), and FeO (0–0.3 wt %) concentrations in analyzed coffinites from the both uranium ore deposits.

In altered granodiorites uraninite occurs usually as isolated small grains of 5–20  $\mu\text{m}$  diameter (Figure 8d). The  $\text{UO}_2$  content in uraninite is relatively high, 80.4–81.9 wt %. Uraninite is partly enriched in  $\text{ThO}_2$  (up to 9.8 wt %) and in  $\text{Y}_2\text{O}_3$  (up to 2.8 wt %) (Table 2, Figures 11 and 12). Concentrations variability of all other constituents is relatively small: the CaO content varies from 0.1 to 0.5 wt %, the FeO from 0.2 to 0.3 wt % and the  $\text{SiO}_2$  from 0.0 to 0.2 wt %. Partly higher is variability of the PbO concentrations, from 0.0 to 4.1 wt %.

Thorite occurs usually as isolated grains, in size from 50 to 100  $\mu\text{m}$  (Figure 8e). For analyzed thorite the variations of the  $\text{UO}_2$  content is significant (1.5–16.9 wt %) (Figure 11). The variability of the all other components is partly lower: the CaO content varies from 0.9 to 4.1 wt %, the  $\text{SiO}_2$  from 17.2 to 19.5 wt %, the  $\text{ZrO}_2$  from 0 to 5.7 wt %, the FeO from 0.4 to 3.6 wt %, the  $\text{P}_2\text{O}_5$  from 0.6 to 1.8 wt %, and the  $\text{TiO}_2$  from 0 to 0.2 wt %.

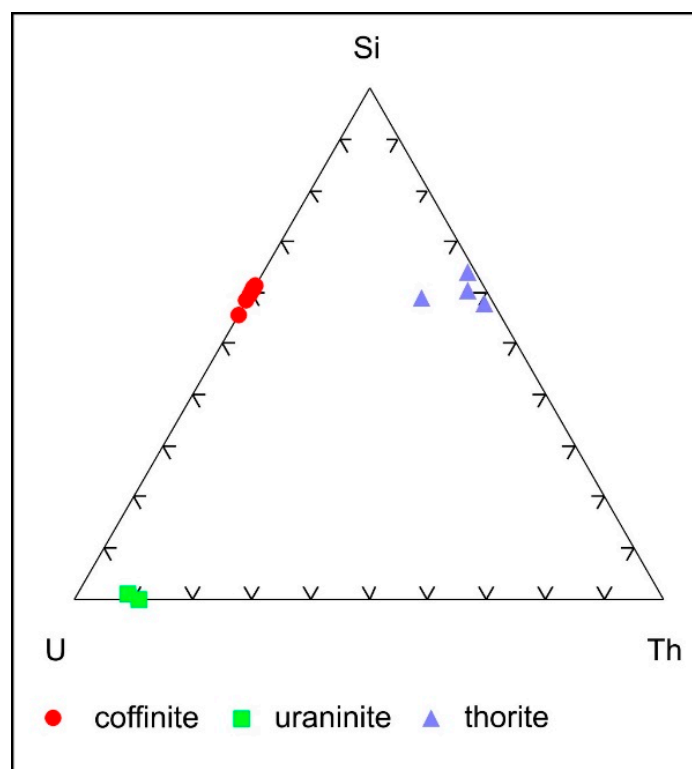


**Figure 11.** Composition of coffinite, uraninite, and thorite from the Nahošín and Mečichov uranium deposits.

**Table 2.** Representative analyses of uranium and thorium minerals (wt %).

Sample	R-752-17	R752-19	R-752-20	R-752-21	R-784-30	R-787-20	R-784-43
Locality	Nahošín	Nahošín	Nahošín	Nahošín	Mečichov	Mečichov	Mečichov
Mineral	coffinite	coffinite	coffinite	coffinite	thorite	thorite	uraninite
UO <sub>2</sub>	60.99	61.64	61.50	59.48	1.85	4.70	81.90
ThO <sub>2</sub>	b.d.l.	b.d.l.	0.01	b.d.l.	54.94	51.71	9.78
TiO <sub>2</sub>	0.91	1.32	0.21	0.35	b.d.l.	0.17	b.d.l.
FeO	0.05	0.12	0.13	0.26	2.14	0.65	0.28
CaO	1.57	1.49	1.39	1.73	1.19	0.97	0.08
MnO	b.d.l.	0.02	b.d.l.	0.04	n.d.	n.d.	n.d.
SiO <sub>2</sub>	21.08	21.07	20.95	20.82	17.78	19.46	b.d.l.
ZrO <sub>2</sub>	b.d.l.	0.15	0.97	0.19	0.16	1.31	b.d.l.
Nb <sub>2</sub> O <sub>5</sub>	0.01	0.03	0.05	0.05	0.04	b.d.l.	b.d.l.
Al <sub>2</sub> O <sub>3</sub>	1.45	1.68	1.53	1.54	0.51	1.33	n.d.
PbO	n.d.	n.d.	n.d.	n.d.	0.55	0.54	4.07
P <sub>2</sub> O <sub>5</sub>	0.25	0.16	0.19	0.20	1.80	0.85	n.d.
La <sub>2</sub> O <sub>3</sub>	0.35	0.38	0.39	0.23	0.22	0.40	b.d.l.
Ce <sub>2</sub> O <sub>3</sub>	2.44	2.16	2.05	1.92	1.20	1.45	0.26
Pr <sub>2</sub> O <sub>3</sub>	0.57	0.41	0.42	0.35	n.d.	n.d.	b.d.l.
Nd <sub>2</sub> O <sub>3</sub>	2.54	1.96	1.50	2.22	n.d.	n.d.	0.49
Sm <sub>2</sub> O <sub>3</sub>	0.60	0.58	0.61	1.01	n.d.	n.d.	0.04
Gd <sub>2</sub> O <sub>3</sub>	0.49	0.56	0.64	0.80	n.d.	n.d.	0.05
Dy <sub>2</sub> O <sub>3</sub>	0.30	0.26	0.47	0.65	0.69	0.63	0.21
Er <sub>2</sub> O <sub>3</sub>	0.07	0.16	0.23	0.37	0.33	0.05	0.08
Yb <sub>2</sub> O <sub>3</sub>	0.04	0.14	0.24	0.24	0.42	0.17	b.d.l.
Y <sub>2</sub> O <sub>3</sub>	2.27	2.03	2.86	3.06	4.35	3.12	1.01
Total	96.70	96.95	96.34	95.51	87.49	87.51	98.25

n.d.—no determined, b.d.l.—below detection limit.

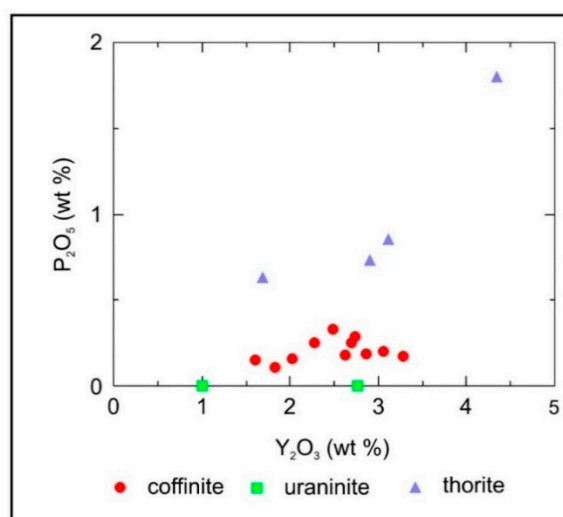


**Figure 12.** Plot of  $P_2O_5$  vs.  $Y_2O_3$  for coffinite, uraninite, and thorite from the Nahošín and Mečichov uranium deposits.

#### 4.6. Composition of REE-Fluorcarbonates

Some cavities and cracks in the highly altered biotite granodiorites from the Nahošín and Mečichov uranium deposits are filled by fine-grained aggregates of REE-fluorcarbonates (Figure 8a,b). These interstitial fillings very probably formed during the post-ore stage, together with fillings of calcite. The microprobe data of these REE-fluorcarbonates show that analyzed REE fluorcarbonates correspond to synchysite-(Ce) (Table 3). All analyzed grains in bigger, fine-grained synchysite aggregates are LREE-dominant with La/Ce ratio of 0.48–0.59. The LREE are presented in concentrations of 45.4–50.7 wt %. The sum of analyzed HREE (Gd and Dy) is only 0.4–1.0 wt %. The concentrations of Y are also low (0.3–0.5 wt %  $Y_2O_3$ ). The analyzed synchysite grains display very low Th concentrations (0.3–1.0 wt %  $ThO_2$ ). Concentrations of F are near of stoichiometric formulae of synchysite (6 wt % F)—5.2–6.0 wt %. In synchysite microprobe analyses, the ratio of Ca versus the other detected cations is near to 1:1 (0.88/1.06), as predicted from its ideal stoichiometry.

**Table 3.** Representative chemical analyses of synchysite (wt %).

Analyte	R-784-27	R-784-33	R-784-34	R-784-36
Locality	Mečichov	Mečichov	Mečichov	Mečichov
$SO_3$	0.10	b.d.l.	0.05	0.11
$P_2O_5$	0.46	0.00	0.03	0.93
$As_2O_5$	b.d.l.	b.d.l.	0.11	0.22
$CO_2^*$	24.98	28.18	27.59	25.87
$SiO_2$	1.40	0.08	0.10	0.17
$ThO_2$	0.95	0.28	0.39	0.70
$UO_2$	0.03	b.d.l.	b.d.l.	0.05
$Y_2O_3$	0.47	0.29	0.43	0.32
$La_2O_3$	10.38	14.61	12.76	12.10
$Ce_2O_3$	21.83	25.06	24.56	25.08
$Pr_2O_3$	2.48	2.36	2.44	2.46
$Nd_2O_3$	11.41	8.08	7.84	8.73
$Sm_2O_3$	1.91	0.58	0.86	0.68
$Eu_2O_3$	b.d.l.	0.02	0.04	b.d.l.
$Gd_2O_3$	0.82	0.26	0.33	0.30
$Dy_2O_3$	0.20	0.10	0.07	0.08
FeO	0.68	b.d.l.	0.33	1.20

Table 3. Cont.

Analyze	R-784-27	R-784-33	R-784-34	R-784-36
Locality	Mečichov	Mečichov	Mečichov	Mečichov
CaO	15.99	18.39	18.16	15.96
SrO	b.d.l.	b.d.l.	b.d.l.	b.d.l.
BaO	b.d.l.	b.d.l.	b.d.l.	b.d.l.
PbO	0.04	0.03	b.d.l.	0.03
H <sub>2</sub> O *	0.03	0.04	0.01	0.11
F	5.62	6.02	5.97	5.54
O=F	−2.36	−2.53	−2.51	−2.33
Total	97.22	101.85	99.56	98.31
Ca/cations	0.91	1.04	1.06	0.88
La/Ce	0.48	0.59	0.52	0.49
La/Nd	0.94	1.87	1.68	1.43

b.d.l.—below detection limit, CO<sub>2</sub> \*, H<sub>2</sub>O \*—calculated according stoichiometry.

## 5. Discussion

### 5.1. Origin and Evolution of Aceites

The recent IUGS classification of metasomatic rocks distinctly delimited the low-temperature albitization (aceitization) with significant removing of original magmatic quartz and high-temperature fault-related alkaline metasomatism with typical occurrence of alkali amphiboles and pyroxenes [11]. The low-temperature hydrothermal alterations characteristics of disseminated uranium deposits of the Massif Central and Armorican Massif, France were in the past described as episyenites (e.g., [8–10]). However, according to the recent IUGS classification for metasomatic rocks [11], these low-temperature metasomatic rocks could be named as aceites, and the term episyenite could be abandoned. The term aceite was introduced to geosciences by Omel'yanenko [12].

Three and/or four stages of hydrothermal alteration can be distinguished in uranium deposits bound by brittle shear zones developed in granitoids of the Bohemian Massif [2,3,5]. Usually, the pre-ore, ore, and post-ore stages are distinguished. The pre-ore stage is represented mainly by chlorite I and albite, which originated by chloritization of biotite and albitization of original plagioclases. The albitization is sometimes accompanied by K-feldspathization and by formation of fine-grained muscovite (sericite) aggregates. The strongest hydrothermal alteration of the original granitoids is accompanied by the formation of fine-grained aggregates of hematite, usually occurring in albite. The uranium minerals (uraninite and coffinite) are the main minerals of the ore-stage. The post-ore stage is coupled with origin of carbonates (predominantly calcite), quartz, and clay minerals (illite, kaolinite, and smectite). The post-ore stage is also significant for the origin of sulfides (pyrite, chalcopyrite, and galena), rare REE-fluorcarbonates, and/or selenides.

The differences in mineralogical composition of original granitoids (S-type two-mica granites, biotite granites, and I-type granodiorites) are expressed by the different mineralogical composition, textural features, and geochemistry of aceites [3,8,10]. The most significant textural features of aceites evolved in granitic rocks is origin of cavities originated by leaching of original magmatic quartz coupled with origin of hematite framework. Hydrothermal altered granitoids have thus distinctly higher porosity than original magmatic rocks.

### 5.2. Sources of Uranium and Thorium

Uranium and thorium in unaltered granodiorites of this area are essentially hosted in accessory minerals, especially in zircon and allanite. Therefore, the distribution of both the radioactive elements in the following ore minerals (uraninite, coffinite, and thorite) could be coupled with hydrothermal alteration/decomposition of the above-mentioned accessory minerals. Similar sources of uranium were

proposed for the unconformity-type uranium deposits in Canada [29] and also for the Nahošín uranium deposit [19]. However, according to Litochleb et al. [19], the significant source of uranium in uranium mineralization could be also hydrothermal alteration of original magmatic biotite, which in some cases contains higher concentrations of uranium (up to 15 ppm U), which is adsorbed on their flakes. During alteration of biotite to chlorite this uranium was mobilized in the hydrothermal solutions.

### 5.3. Behavior of Yttrium and Zirconium

Yttrium and Zr are typical high field strength elements (HFSE), which are generally considered immobile during hydrothermal processes [30]. Some experimental data, however, have demonstrated that the both elements may be mobile in hydrothermal environments [31,32]. The mobility of yttrium in aegirites from the Nahošín and Mečichov uranium deposits is suggested from the occurrence of Y-enriched coffinite, uraninite and thorite in the both uranium deposits. Similar Y-enriched coffinite with up to 3.4 wt %  $Y_2O_3$  was found in the Okrouhlá Radouň uranium deposit, evolved in two-mica granites of the Moldanubian batholith [2]. The Y-enriched coffinites and uraninites are worldwide relatively rare. However, coffinite from the Olympic Dam uranium deposit, Australia, contains up to 15.6 wt %  $Y_2O_3$  [33] and coffinite from the albitized biotite granites, Ririway, Nigeria contains up to 15.9 wt %  $Y_2O_3$  [34]. Coffinite enriched in Y and Zr, together with occurrence of the U-Zr-Si mixed phases has also been found in the Mount Isa uranium deposit in Australia [35]. The Y-enriched uraninite was described by Shahin [36] from Gabal Gattar uranium deposit in Egypt, containing up to 3.3 wt %  $Y_2O_3$ . The Y-enriched uraninite occurring in the Olympic Dam uranium deposit, Australia contains up to 3.6 wt %  $Y_2O_3$  [33]. Recently the Y-bearing uraninite was described from the high-temperature Na-metasomatic uranium deposit Jiling, NW-China, containing 1.0–2.5 wt %  $Y_2O_3$  [37]. However, all these Y-enriched uraninites and coffinites occur in a high-temperature albitites, which originated by distinctly higher temperatures than the low-temperature aegirites [11,33,35,37,38].

### 5.4. Occurrence of Th-Rich Uraninite and Thorite

Th-rich uraninites and thorites from hydrothermal uranium deposits are relatively rare minerals. The Th-enriched uraninite, containing up to 7.3 wt %  $ThO_2$  was described from uranium deposit Aricheng in Guyana, occurring in high-temperature albitites [38]. Similar, the Jiling uranium deposit in the NW-China contains Th-enriched uraninite with 6.5–12.6 wt %  $ThO_2$  [37]. The Th-enriched uraninite from the Olympic Dam uranium deposit in Australia contains up to 7.4 wt %  $ThO_2$  [33]. However, the concentrations of Th in uraninite from uranium ore deposits of the Bohemian Massif are very low. Uraninite from the Jáchymov uranium deposit contains only up to 0.08 wt %  $ThO_2$  and uraninite from the Příbram uranium deposit contains up to 0.09 wt %  $ThO_2$  [6].

Occurrence of thorite from hydrothermal uranium deposits is mentioned by Freemantle [39] from the U-deposits in the Central Damara Orogen, Namibia. Another occurrence mentioned from this area is the presence of Th-rich uraninite and Y-bearing thorite. The Th-rich uraninite from the prominent Husab uranium deposit contains 7.3–9.4 wt %  $ThO_2$ . The Zr-enriched thorite containing 2.9–26.8 wt %  $ZrO_2$  is mentioned from the Um Ara uranium deposit in Egypt [40]. Thorite from the Vale de Abrutiga (Central Portugal) uranium deposit in hydrothermally altered biotite granites contains up to 5.9 wt %  $ZrO_2$  and up to 5.6 wt %  $Y_2O_3$  [41].

### 5.5. Occurrence and Origin of REE-Fluorcarbonates

Synchysite-(Ce) is a relatively highly widespread RE-fluorcarbonate found within different geological environments, especially in carbonatites [42–46], alkali pegmatites [47], altered granitic rocks [48–52], and in ore deposits [53–55]. Synchysite-(Ce) with distinctly more widespread bastnäsite occurs in a world-class breccia-hosted iron-oxide copper-gold-uranium deposit, i.e., Olympic Dam in Australia [55]. As advocated by Fleischer [56], the La/Nd ratio in synchysite could be used as useful indicator occurrence of synchysite in different geological environments. For its origin from hydrothermal solutions it shows typical values of  $La/Nd = 1.16$  and  $La/Ce = 0.47$  [51,57,58].

The synchysite from the Olympic Dam uranium deposit has  $La/Nd = 1.15$  and  $La/Ce = 0.42$ . Both these values for synchysite from the Mečichov uranium deposit are slightly higher ( $La/Nd = 0.94$ – $1.68$ ,  $La/Ce = 0.48$ – $0.59$ ). However, values of both ratios for synchysite from pegmatites and carbonatites are distinctly higher—pegmatites ( $La/Nd = 1.69$ ,  $La/Ce = 0.52$ ) and carbonatites ( $La/Nd = 2.07$ ,  $La/Ce = 0.62$ ) [43,47,59].

## 6. Conclusions

1. The disseminated coffinite-uraninite-thorite mineralization occurs in highly hydrothermal altered amphibole-bearing biotite granodiorites of the Blatná suite. In intensively hematitized granitoids the content of  $Fe_2O_3$  reaches up to 3.3 wt %. The content of Ca distinctly increases due to intensive carbonatization, reaching up to 14.4 wt % CaO in acceites from the Nahošín deposit. The content of Na increases especially in altered granodiorites from the Mečichov deposit (up to 5.4 wt %  $Na_2O$ ). In granodiorites affected by K-feldspathization, there are distinctly increased K concentrations (up to 6.2 wt %  $K_2O$ ). These granodiorites are also enriched on Rb (up to 214 ppm). In the same acceites depletions in Sr were found (79–383 ppm). The altered granodiorites from the Nahošín deposit occur high Y concentrations (up to 45 ppm).
2. Coffinite, uraninite, and thorite is distinctly enriched in Y (up to 4.3 wt % in thorite). Uraninite is enriched in Th (up to 9.8 wt %  $ThO_2$ ) and thorite is enriched also in Zr (up to 5.7 wt %  $ZrO_2$ ). The enrichment of the both elements in above mentioned uranium minerals very probably correlated with their enrichment in original I-type granitic rocks.
3. In the highly carbonatized acceites from the Mečichov uranium deposit REE-fluorcarbonate synchysite—(Ce) was found with  $La/Nd = 2.07$  and  $La/Ce = 0.62$ . The REE-fluorcarbonates are in uranium deposits very rare and their occurrence in researched uranium deposits is the first occurrence in acceites.

**Supplementary Materials:** The following are available online <http://www.mdpi.com/2075-163X/10/9/821/s1>, Table S1: List of used samples and their localization, petrography, and geochemistry.

**Funding:** This research received no external funding.

**Acknowledgments:** The research for this paper was carried out thanks to the support of the long-term conceptual development research organization RVO 67985891. I would like to Z. Škoda and J. Haifler from the Masaryk University Brno for the technical help with the microprobe measurements. Three anonymous reviewers and the journal editor are thanked for their perceptive reviews of the manuscript, valuable comments, and recommendations.

**Conflicts of Interest:** The author declares no conflict of interest.

## References

1. Kříbek, B.; Žák, K.; Dobeš, P.; Leichmann, J.; Pudilová, M.; René, M.; Scharm, B.; Scharmová, M.; Hájek, A.; Holeczy, D. The rožná uranium deposit (Bohemian Massif, Czech Republic): Shear-zone hosted, late variscan and post-variscan hydrothermal mineralization. *Minim. Depos.* **2009**, *44*, 99–128. [CrossRef]
2. René, M. Rare earth, yttrium and zirconium mobility associated with the uranium mineralization at okrouhlá radouň, bohemian massif, Czech Republic. *Eur. J. Mineral.* **2015**, *27*, 57–70. [CrossRef]
3. René, M. Alteration of granitoids and crystalline rocks and uranium mineralization in the bor pluton area, bohemian massif, Czech Republic. *Ore Geol. Rev.* **2017**, *81*, 188–200. [CrossRef]
4. René, M. Shear Zone-Hosted Uranium Deposits of the Bohemian Massif (Central European Variscan Belt). In *Uranium-Safety, Resources, Separation and Thermodynamic Calculation*; Awwad, N.S., Ed.; IntechOpen Ltd.: London, UK, 2018; pp. 49–64. [CrossRef]
5. René, M.; Dolníček, Z. Uraninite, coffinite and brannerite from shear-zone hosted uranium deposits of the Bohemian Massif (Central European Variscan Belt). *Minerals* **2017**, *7*, 50. [CrossRef]
6. René, M.; Dolníček, Z.; Sejkora, J.; Škacha, P.; Šrein, V. Uraninite, coffinite and ningyoite from vein-type uranium deposits of the Bohemian Massif (Central European Variscan Belt). *Minerals* **2019**, *9*, 123. [CrossRef]

7. Havelcová, M.; Machovič, V.; René, M.; Sýkorová, I.; Lapčák, L.; Špaldoňová, A. Geochemistry of shear-hosted uranium mineralization at the Zadní Chodov uranium deposit (Bohemian Massif). *Ore Geol. Rev.* **2020**, *120*, 1–16. [[CrossRef](#)]
8. Cathelineau, M. The hydrothermal alkali metasomatism effects on granitic rocks. Quartz dissolution and related subsolidus changes. *J. Pets* **1986**, *27*, 945–965. [[CrossRef](#)]
9. Leroy, J. The Margnac and Fanay uranium deposits of the La Crouzille district (western Massif Central, France): Geologic and fluid inclusion studies. *Econ. Geol.* **1978**, *73*, 1611–1634. [[CrossRef](#)]
10. Suikkanen, E.; Rämö, O.T. Episyenites-Characteristics, genetic constraints, and mineral potential. *Min. Met. Explor.* **2019**, *36*, 1–18. [[CrossRef](#)]
11. Fettes, D.; Desmons, J. (Eds.) *Metamorphic Rocks: A Classification and Glossary of Terms: Recommendations of the International Union of Geological Sciences. Subcommission on the Systematics of Metamorphic Rocks*; Cambridge University Press: Cambridge, UK, 2007; p. 244.
12. Omel'yanenko, B.I. *Wall-Rock Hydrothermal Alterations*; Nedra Publishing House: Moscow, Russia, 1978; pp. 1–215. (In Russian)
13. Janoušek, V.; Bowes, D.R.; Rogers, G.; Farrow, C.M.; Jelínek, E. Modelling diverse processes in the petrogenesis of a composite batholith: The central bohemian pluton, central european variscides. *J. Pets* **2000**, *41*, 511–543. [[CrossRef](#)]
14. Janoušek, V.; Wiegand, B.A.; Žák, J. Dating the offset of Variscan crustal exhumation in the core of the bohemian massif: New U Pb single zircon ages from the high-K calc alkaline granodiorites of the Blatná suite, Central Bohemian Plutonic Complex. *J. Geol. Soc.* **2010**, *167*, 347–360. [[CrossRef](#)]
15. Žák, J.; Verner, K.; Holub, F.V.; Kabele, P.; Chlupáčová, M.; Halodová, P. Magmatic to solid state fabrics in syntectonic granitoids recording early carboniferous orogenic collapse in the bohemian massif. *J. Struct. Geol.* **2012**, *36*, 27–42. [[CrossRef](#)]
16. Habásko, J.; Litochleb, J.; Pletánek, Z. The new findings about uranium mineralization in granitoids of the SW part of the central bohemian pluton. In *Sbor. Symp. Horn. Příbram ve Vědě a Technice, Geologie*; ČSÚP: Příbram, Czech Republic, 1980; pp. 67–87. (In Czech)
17. Litochleb, J.; Novická, Z.; Hlaváček, A. Mineralogical-petrological and geochemical characteristics of uranium mineralization and hydrothermal altered rocks on the Nahošín and Mečichov uranium deposits. *Uranium Explor. Enterp. Příbram.* **1984**, unpublished report. 1–101. (In Czech)
18. Litochleb, J.; Kotlovský, P. Geological building and mineralization of the nahošín uranium deposit. In *Sbor. Symp. Horn. Příbram ve vědě a Technice*; ČSÚP: Příbram, Czech Republic, 1988; pp. 91–101. (In Czech)
19. Litochleb, J.; Sejkora, J.; Šrein, V.; Klauudy, S.; Cílek, V.; Žák, K. Hydrothermal alterations and mineralization of the uranium deposit Nahošín SW of Blatná, Czech Republic. *Bull. Mineral. Petrogr. Odd. Nár. Muz. (Praha)* **2009**, *17*, 1–22. (In Czech)
20. René, M. Petrogenesis of granitoids of the Blatná area. *Acta Mont.* **1998**, *12*, 141–152.
21. René, M. Petrogenesis of granitoids of the Červená type (central bohemian plutonic complex). *Acta Mont. IRSM AS CR* **1999**, *14*, 81–97.
22. Dudek, A.; Fediuk, F. Quarries for granodiorite in environs of Blatná. *Geotechnica* **1960**, *30*, 1–63. (In Czech)
23. DIAMO. *The Mining and Mining Possibilities of Uranium in the Czech Republic*; DIAMO: Stráž pod Ralskem, Czech Republic, unpublished study. (In Czech)
24. Kafka, J. (Ed.) *Czech Ore and Uranium Mining Industry*; Anagram: Ostrava, Czech Republic, 2003; pp. 1–647. (In Czech)
25. Grant, J.A. The isocon diagram-A simple solution to gresens equation for metasomatic alteration. *Econ. Geol.* **1986**, *81*, 1976–1982. [[CrossRef](#)]
26. Pouchou, J.J.; Pichoir, F. "PAP" ( $\phi$ - $\rho$ -Z) procedure for improved quantitative microanalysis. In *Microbeam Analysis*; Armstrong, J.T., Ed.; San Francisco Press: San Francisco, CA, USA, 1985; pp. 104–106.
27. Collins, W.J.; Beams, S.D.; White, A.J.R.; Chappell, B.W. Nature and origin of A-type granites with particular reference to southeastern Australia. *Contrib. Miner. Pets* **1982**, *80*, 189–200. [[CrossRef](#)]
28. Whalen, J.B.; Currie, K.L.; Chappell, B.W. A-type granites: Geochemical characteristics, discrimination and petrogenesis. *Contrib. Miner. Pets* **1987**, *95*, 407–419. [[CrossRef](#)]
29. Hecht, L.; Cuney, M. Hydrothermal alteration of monazite in the precambrian crystalline basement of the athabasca basin (Saskatchewan, Canada): Implications for the formation of unconformity-related uranium deposits. *Minim. Depos.* **2000**, *35*, 791–795. [[CrossRef](#)]

30. Bau, M. Controls on the fractionation of isovalent trace elements in magmatic and igneous systems: Evidence from Y/Ho, Zr/Hf and lanthanide tetrad effect. *Contrib. Miner. Pets* **1996**, *123*, 323–333. [[CrossRef](#)]
31. Gière, R. Transport and deposition of REE in H<sub>2</sub>S-rich fluids: Evidence from accessory mineral assemblages. *Chem. Geol.* **1993**, 251–268. [[CrossRef](#)]
32. Rubin, J.W.; Henry, C.D.; Price, J.G. The mobility of zirconium and other “immobile” elements during hydrothermal alteration. *Chem. Geol.* **1993**, *110*, 29–47. [[CrossRef](#)]
33. MacMillan, E.; Cook, N.J.; Ehrig, K.; Pring, A. Chemical and textural interpretation of large stage coffinite and brannerite from the Olympic dam IOCG-Ag-U deposit. *Miner. Mag.* **2017**, *81*, 1323–1368. [[CrossRef](#)]
34. Pointer, C.M.; Asworth, J.R.; Ixer, R.A. The zircon-thorite mineral group in metasomatized granite, ririwai, nigeria. 1. Geochemistry and metastable solid solution in thorite and coffinite. *Miner. Pets* **1988**, *38*, 245–262. [[CrossRef](#)]
35. Wilde, A.; Otto, A.; Jory, J.; MacRae, C.; Pownceby, M.; Wilson, N.; Torby, A. Geology and mineralogy of uranium deposits from Mount Isa, Australia: Implications for albitite uranium deposit model. *Minerals* **2013**, *3*, 258–283. [[CrossRef](#)]
36. Shahin, A.A. Geochemical characteristics and chemical electron microprobe U-Pb-Th dating of pitchblende mineralization from gabal gattar younger granite, north eastern desert, Egypt. *Open J. Geol.* **2014**, *4*, 24–32. [[CrossRef](#)]
37. Yu, C.; Wang, K.; Liu, X.; Cuney, M.; Pan, J.; Wang, G.; Zhang, L.; Zhang, J. Uranium mineralogical and chemical features of the Na-metasomatic type uranium deposit in the Longshoushan metallogenic belt, northwestern China. *Minerals* **2020**, *10*, 335. [[CrossRef](#)]
38. Alexandre, P. Mineralogy and geochemistry of the sodian metasomatism-related uranium occurrence of Aricheng South, Guyana. *Minim. Depos.* **2015**, *45*, 351–367. [[CrossRef](#)]
39. Freemantle, G.G. Primary Uranium Mineralization of the Central Damara Orogeny, Namibia. Ph.D. Thesis, University of Witwatersrand, Johannesburg, South Africa, 2015.
40. Abd El-Naby, H.H. High and low temperature alteration of uranium and thorium minerals, Um Ara granites, south eastern desert, Egypt. *Ore Geol. Rev.* **2009**, *35*, 436–446. [[CrossRef](#)]
41. Cabral Pinto, M.M.S.; Silva, M.M.V.G.; Neiva, A.M.R.; Guimarães, F.; Silva, P.B. Release, migration, sorption and (re)precipitation of U during peraluminous granite alteration under oxidizing conditions in Central Portugal. *Geosciences* **2018**, *8*, 95. [[CrossRef](#)]
42. Hogarth, D.D.; Hartree, R.; Loop, J.; Solberg, T.N. Rare-earth element minerals in four carbonatites near Gatineau, Quebec. *Amer. Miner.* **1985**, *70*, 1135–1142.
43. Zaitsev, A.N.; Wall, F.; Le Bas, M.J. REE-Sr-Ba minerals from the Khibina carbonatites, Kola Peninsula, Russia: Their mineralogy, paragenesis and evolution. *Miner. Mag.* **1998**, *62*, 225–250. [[CrossRef](#)]
44. Smith, M.P.; Henderson, P.; Campbell, L.S. Fractionation of the REE during hydrothermal processes: Constraints from the Bayan Obo Fe-REE-Nb deposit, Inner Mongolia, China. *Geochim. Cosmochim. Acta* **2000**, *64*, 3141–3160. [[CrossRef](#)]
45. Yang, X.; LeBas, M.J. Chemical composition of carbonate minerals from Bayan Obo, Inner Mongolia, China: Implications for petrogenesis. *Lithos* **2004**, *72*, 97–116. [[CrossRef](#)]
46. Ruberti, E.; Enrich, G.E.R.; Gomes, C.B.; Comin-Chiaramonti, P. Hydrothermal REE fluorocarbonate mineralization at Barra do itapirapuã, a multiple stockwork carbonatite, Southern Brazil. *Can. Miner.* **2008**, *46*, 901–914. [[CrossRef](#)]
47. Guastoni, A.; Nestola, F.; Giaretta, A. Mineral chemistry and alteration of rare earth element (REE) carbonates from alkali pegmatites of Mount Malosa, Malawi. *Am. Miner.* **2009**, *94*, 1216–1222. [[CrossRef](#)]
48. Littlejohn, A.L. Alteration products of accessory allanite in radioactive granites from the Canadian shield. *Geol. Surv. Can. Pap.* **1981**, *81*, 95–104.
49. Caruso, L.; Simmons, G. Uranium and microcracks in a 1.000-meter core, redstone, new hampshire. *Contrib. Miner. Pets* **1985**, *90*, 1–17. [[CrossRef](#)]
50. Johan, Z.; Johan, V. Accessory minerals of the cinovec (zinnwald) granite cupola, Czech Republic: Indicators of petrogenetic evolution. *Miner. Pets* **2005**, *83*, 113–150. [[CrossRef](#)]
51. Förster, H.-J. Cerite-(Ce) and thorian synchysite-(Ce) from niederbobritzsch (Erzgebirge, Germany): Implications for the differential mobility of Th and the LREE during granite alteration. *Can. Miner.* **2000**, *38*, 67–79. [[CrossRef](#)]

52. Förster, H.-J. Synchysite-(Y)-synchysite-(Ce) solid solutions from markersbach, Erzgebirge, Germany: REE and Th mobility during high-T alteration of highly fractionated aluminous A-type granites. *Miner. Pets* **2001**, *72*, 259–280. [[CrossRef](#)]
53. Lottermoser, B.G. Rare earth element mineralogy of the olympic dam Cu-U-Au-Ag deposit, roxby downs, South Australia: Implications for ore genesis. *Neues. Jahrb. Miner. Mon.* **1995**, *8*, 371–384.
54. Capitani, G. Synchysite-(Ce) from Cinqueralli (Tronto, Italy): Stacking disorder and polytypism of (Ca, REE)-fluorocarbonates. *Minerals* **2020**, *10*, 77. [[CrossRef](#)]
55. Schmandt, D.S.; Cook, N.J.; Ciobanu, C.L.; Ehrig, K.; Wade, B.P.; Gilbert, S.; Kamenetsky, V.S. Rare earth element fluorocarbonate minerals from the olympic dam Cu-U-Au-Ag deposit, south Australia. *Minerals* **2017**, *7*, 202. [[CrossRef](#)]
56. Fleischer, M. Relative proportions of the lanthanides in minerals of the bastnaesite group. *Can. Miner.* **1978**, *16*, 361–363.
57. Grammatikoupolos, T.; Mercer, W.; Gunning, C.; Prout, S. Quantitative characterization of the REE minerals by QEMSCAN from nechalacho heavy rare earth deposit, Thor Lke prospect, NWT, Canada. *SGS Miner. Surv. Tech. Pap.* **2011**, *7*, 1–11.
58. Papoutsas, A.; Pe-Piper, G. Variation of REE-Hydrothermal circulation in complex shear zones: The cobequid highland, Nova Scotia. *Can. Miner.* **2014**, *52*, 943–968. [[CrossRef](#)]
59. Broom-Fendley, S.; Brady, A.E.; Wall, F.; Gunn, G.; Dawes, W. REE minerals at the songwe hill carbonatite, malawi: HREE-enrichment in late-stage apatite. *Ore Geol. Rev.* **2017**, *81*, 23–41. [[CrossRef](#)]



© 2020 by the author. Licensee MDPI, Basel, Switzerland. This article is an open access article distributed under the terms and conditions of the Creative Commons Attribution (CC BY) license (<http://creativecommons.org/licenses/by/4.0/>).